Basarir, Fevzihan; Madani, Zahra; Vapaavuori, Jaana

Recent Advances in Silver Nanowire Based Flexible Capacitive Pressure Sensors: From Structure, Fabrication to Emerging Applications

Published in:
Advanced Materials Interfaces

DOI:
10.1002/admi.202200866

Published: 01/11/2022

Document Version
Publisher's PDF, also known as Version of record

Please cite the original version:
Basarir, F., Madani, Z., & Vapaavuori, J. (2022). Recent Advances in Silver Nanowire Based Flexible Capacitive Pressure Sensors: From Structure, Fabrication to Emerging Applications. *Advanced Materials Interfaces*, *9*(31), Article 2200866. https://doi.org/10.1002/admi.202200866

ADVANCED MATERIALS INTERFACES
www.advmatinterfaces.de

Recent Advances in Silver Nanowire Based Flexible Capacitive Pressure Sensors: From Structure, Fabrication to Emerging Applications

*Fevzihan Basarir, Zahra Madani, and Jaana Vapaavuori**

Skin mountable flexible pressure sensors are crucial for the next generation technologies. Capacitive pressure sensors bring several advantages and hence, they have been preferred over piezoelectric and piezoresistive alternatives. Flexible electrode and dielectric material are the fundamental components of the capacitive flexible pressure sensors. Hence, solution processable silver nanowires (AgNWs) are highly promising as electrode material or filler material in dielectric layer, owing to their superior inherent conductivity and flexibility. This article reviews recent progress on fabrication of flexible capacitive pressure sensors with AgNWs used as electrode and dielectric material. Performance of the sensors based on AgNWs is comprehensively discussed and emerging applications, as well as future outlook, are presented in detail.

1. Introduction

In the last decade, considerable research effort has been dedicated to flexible pressure sensors since they have wide uses in electronic skin,[1] human–machine interaction,[2] human motion detection,[3] healthcare monitoring[4,5] and soft robots.[6] Based on the working mechanism, pressure sensors can be classified as piezoelectric, piezoresistive and capacitive sensors.[7,8] Among those, capacitive sensors bring advantages of higher accuracy, less power consumption, and less dependence on external conditions, such as temperature and humidity.[9,10] On the other hand, low power organic field-effect transistor (OFET) pressure sensors are extremely promising in the futuristic applications such as artificial skin and soft bioelectronics.[11–13] The capacitive pressure sensor market is forecasted to reach 4 billion USD by 2026 and has found several applications in various industries.[14] However, the entry of flexible capacitive pressure sensor to market is in its infancy stage.

Conventional capacitive sensors consist of two parallel plate electrodes with a dielectric interlayer sandwiched in between. Electrically conductive electrode and dielectric layer are the core elements of a flexible pressure sensors.[9,10] The electrode should be flexible and bendable; however, the conventional inorganic films do not meet these requirements.[15] Therefore, solution processable nanomaterials including carbon nanotubes,[16,17] graphene,[18,19] Mxenes[20,21] and silver nanowires (AgNWs)[22,23] have been taken into consideration in the literature. Owing to their high inherent conductivity, excellent flexibility, and resistance to oxidation, AgNWs are concluded to have multiple distinct advantages as compared to other nanomaterials. Hence, several approaches have been demonstrated in the scientific literature for the fabrication of AgNW based electrodes[23–27] although the commercial penetration of AgNW-based electrodes is still limited. Since AgNWs are one of the most employed and promising conductive nanomaterial used in fabrication of flexible sensors, it is important to understand how the properties of AgNWs can be influenced by various strategies used to synthesize them. The outstanding properties of AgNWs include high optical transmission, great flexibility, and high electrical and thermal conductivity.[28,29] In addition to their use in sensors, they can be used in many other applications, such as transparent conducting electrodes,[30,31] thin film heater,[32] organic photovoltaics,[33–35] polymer composites,[36] photocatalysis,[37] microelectronics,[38] and biological sensors.[39]

In a typical process, AgNWs are deposited on a flexible substrate to fabricate the electrodes and a flexible dielectric layer is sandwiched between the electrodes for the construction of the sensors, as illustrated in **Figure 1**. Applied pressure gives rise to thickness reduction of the dielectric layer, which in turn leads to a change in the capacitance of the entire system. In addition to the change of the thickness, the change in the dielectric constant with pressure can also induce a change in the capacitance of the system. Therefore, dielectric layers with controlled amount of AgNWs have been presented by different research groups to enhance the sensitivity and response range.[40,41]

The aim of this literature review is to summarize how it is possible to produce AgNW-based electrodes and dielectric layers, and how these structures can be integrated to fabricate pressure sensors. Additionally, we identify the sensor properties of such devices and highlight the emerging applications. Finally, we discuss the outlook on the future of this technology.

F. Basarir, Z. Madani, J. Vapaavuori
Department of Chemistry and Materials Science
Aalto University
P.O. Box 16100, AALTO FI-00076, Finland
E-mail: jaana.vapaavuori@aalto.fi

The ORCID identification number(s) for the author(s) of this article can be found under https://doi.org/10.1002/admi.202200866.

DOI: 10.1002/admi.202200866

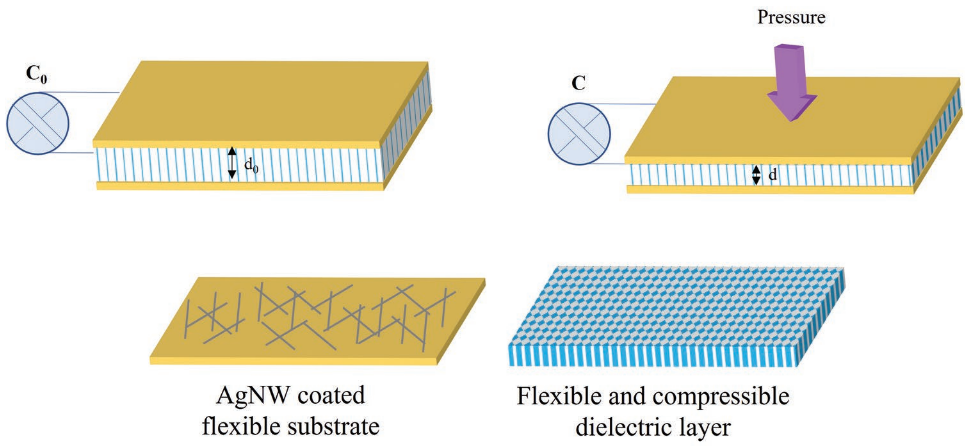

Figure 1. Schematic demonstration of capacitive pressure sensor working mechanism.

2. Flexible Capacitive Pressure Sensors

Typically, flexible capacitive pressure sensors comprise sandwiching a flexible dielectric layer between two flexible electrodes. In this section, we will investigate the components of AgNW based flexible capacitive pressure sensors as well as the sensing mechanism of the sensor.

2.1. Principle of Capacitive Sensing

The capacitive sensor usually consists of two parallel plate electrodes with a dielectric interlayer sandwiched in between. The capacitance of the structure can be calculated by

$$C = (\varepsilon A)/d \tag{1}$$

where ε, A, and d are the dielectric permittivity of the interlayer material, effective electrode area and the distance between the two plate electrodes, respectively. It is apparent from Equation (1) that the capacitance change could be simply achieved by a change in either ε, A, or d. However, since the applied pressure mainly influences the ε and d, the capacitance change of the sensors emerges because of the change in ε and d.

2.2. Electrode Substrate Material

Since the AgNWs are solution processable nanomaterial, there is a need of flexible polymeric substrates for deposition/coating of the AgNWs in order to fabricate flexible conductive electrodes. Flat[22,42] or microstructured[23,43] PDMS has been mainly utilized as such substrate, owing to its high elasticity, flexibility, and chemical resistance. Besides that, utilization of printing paper,[44] flexible wood film,[45] cellulose tape,[46] polyurethane film[25] and PET film[47] have also been demonstrated in the literature. Additionally, porous materials such as wool fabric,[48] melamine sponge[49] and porous PDMS[50] have also been explored. Moreover, to add breathability function to the sensor, PVDF nanofiber membrane was employed as substrate material.[21] Flexibility, elasticity compressibility, conformability, moldability, thermal and chemical resistance are the inevitable requirements for an ideal substrate material. Therefore, we believe that novel substrate design and optimization is required for further advancement of flexible pressure sensor field.

2.3. Electrode Formation

AgNWs can be deposited or patterned on diverse substrate materials, discussed in previous subsection, via a variety of techniques. Details of these electrode fabrication methods are discussed comprehensively in Section 4. Overall, it is essential to note that, alongside the other fabrication parameters, AgNW length has a great influence on the conductivity of the electrode.[51] However, this factor has not yet been systematically taken into account in the AgNW sensor research. Furthermore, long term stability of the AgNWs on the chosen substrate is very critical since the sensors will be subjected to many kinds of deformation throughout their lifecycle so adhesion of the AgNWs to the substrate should also be evaluated as one of the key parameters. Moreover, large area coating or printing techniques, as well as other scalability issues, should be explored before the commercialization of the sensors.

2.4. Dielectric Material

The performance of capacitive pressure sensors mainly depends on the geometric change of the dielectric layer with the external pressure. As summarized in **Table 1**, several materials have been employed as dielectric layer in the AgNW based pressure sensors. It is worthy to note that owing to their high compressibility and elasticity, silicone-based elastomers including PDMS and Ecoflex were mainly employed as dielectric material.[22] However, utilization of thin films of PMMA, PVP, PVDF and PI as well as commercial films including Parafilm, 3M VHB and cellulose tape were additionally demonstrated.[23,25,48,52–54] Natural materials such as bamboo leaf[55] and dried rose petal[46] have—on the other hand—been employed owing to their

Table 1. Properties of the sensors prepared with AgNW based electrode.

Electrode type	Dielectric material	AgNW length [μm]	Resistance/ Sheet resistance	Sensitivity [kPa^{-1}] Subtle pressure (1 Pa– 1 kPa)	Low pressure (1–10 kPa)	Medium pressure (10–100 kPa)	Limit of detection [Pa]	Response time [ms]	Loading/ unloading cycle	Refs.
Plain	3 M VHB tape	10	16 Ω sq^{-1}	–	–	–	–	–	10 (1000 kPa)	[25]
	PDMS	20–30	1.7 Ω sq^{-1}	0.124	0.003	–	2	200	–	[22]
	TPU Nanofiber	>10	–	4.2	0.071	–	1.6	26	10 000 (15 kPa)	[26]
	Iontronic film	84.6	–	131.5	11.73	–	1.12	43	7000 (0.47 kPa)	[42]
	Bamboo leaf	–	–	2.08	0.08	0.08	20	500	4000 (5 N)	[55]
	Microstructured PDMS	25	52 Ω sq^{-1}	1.01	0.28	0.15	–	–	5000 (150 kPa)	[45]
Microstructured	PMMA PVP	–	–	3.8	0.8	0.35	15	<150	1500	[23]
	PVDF	8.4	2.6 Ω sq^{-1}	2.94	0.75	–	3	<50	1000 (2 kPa)	[52]
	PDMS	20–30		1.1	0.08	–	1	<1000	2000	[43]
	Colorless PI	>30	10 Ω sq^{-1}	1.194	0.077		0.8	36	100 000 (0.4 kPa)	[53]
	Wood slice/ionic liquid	>5	–	2.09	2.09	–			500 (80 kPa)	[56]
	Dried rose petal	20–50	4.3 Ω sq^{-1}	0.08	≈0.03	<0.01	7	–	5000 (20 kPa)	[46]
	Cellulose tape	20–50	10 Ω	0.0045	≈0.002	≈0.001	–	–	1800 (12.5 kPa)	[54]
Porous	Parafilm	13.4	–	–	–	–	–	–	–	[48]
	Porous PDMS	5–50	–	–	–	–	–	–	–	[50]
	Melamine sponge		10 Ω	1.285	0.108	0.038	0.5	18	42 000 (1 kPa)	[49]
	TPU nanofiber membrane	>10	–	4.2	0.071	–	1.6	26	10 000 (15 kPa)	[26]
Fiber	Ecoflex	20	–	0.096	–	0.0011	1.5	32	10 000 (0.84 and 13.7 kPa)	[27]
	PDMS	50	–	5.49	0.65	0.01	–	75	2000 (0.6 kPa)	[89]
Patterned	Ecoflex	–	–	–	0.00162	0.00162	–	40	–	[90]
	PDMS	>100	54 Ω sq^{-1}	–	0.0004	–	–	–	200 (100 kPa)	[47]
	PDMS	–	–	–	0.0038	0.00029	–	–	–	[91]
	PDMS	30–50	0.4 Ω sq^{-1}	–	–	–	–	–	100 (5 N)	[92]
	ZnO whiskers/PDMS		500 Ω	0.43	0.15	0.07	–	150	1000	[21]

microstructured form and biodegradability. To increase the sensitivity, porous dielectric materials like melamine sponge[49] and nanofiber membrane,[26] and ionic dielectric materials[42,56] were also investigated.

Another way to cause pressure-related capacitance changes is to implement AgNWs into the dielectric medium, since then the dielectric constant of the device can be modulated upon external pressure due to changing number density of AgNWs. Application of AgNW fillers in dielectric layer and the fabrication details as well as the sensor properties will be discussed in detail in Section 5. Choice of dielectric material is very prominent for the sensor sensitivity and working pressure range so further research is highly desirable for developing porous, highly compressible, and flexible materials.

2.5. Performance of the Sensors

2.5.1. Sensitivity

Sensitivity is one of the most important parameters of a pressure sensor defining the range of available applications. The sensitivity of a capacitive sensor is typically calculated with Equation (2) as:

$$S = \frac{(C/C_0)-1}{\Delta P} = \frac{\Delta C}{\Delta P} \tag{2}$$

where S, C, C_0 and ΔP indicate the sensitivity, capacitance after applying pressure, initial capacitance, and pressure change, respectively. Sensitivity of a pressure sensor stands for the relative capacitance change upon applied external pressure and as described in Equation (2), the sensitivity is higher if the capacitance change is higher with the applied external pressure. Typically, there are five different pressure regimes used in sensor performance characterization: 1) ultralow pressure (<1 Pa), 2) subtle pressure (1 Pa–1 kPa), 3) low pressure (1–10 kPa), 4) medium pressure (10–100 kPa) and 5) high pressure (>100 kPa) range.[9] Depending on the application, sensitivity in one or more regimes might be of relevance, however, achieving high sensitivity in subtle, low and medium pressure regimes is very essential for human motion detection and healthcare monitoring. For instance, intraocular and intracranial pressure fall within the subtle pressure regime while heart rate, blood pressure rate, respiration rate, radial artery wave and jugular venous pulses are in the range of low and medium pressures.[3]

2.5.2. Response Time

Response time is also an important indicator for pressure sensor performance. Response time specifies the sensor's response speed to reach the steady state capacitance value after loading the external pressure.

2.5.3. Dynamic Durability

Dynamic durability is another significant performance indicator for the pressure sensors, which shows the sensor's electrical and mechanical stability to long-term pressure loading/unloading cycles.

2.5.4. Limit of Detection

Limit of detection (LOD) can be explained as the minimum pressure that can be detected by the sensor.

3. Synthesis Methods of Silver Nanowires

Various methods of AgNW synthesis have been introduced by many research groups including templat directed approaches,[57–61] electrochemical methods,[62] ultraviolet irradiation,[63–65] photoreduction,[66,67] polyol process,[68–70] solvothermal,[71–73] and hydrothermal methods.[74–76] For instance, synthesis of AgNWs by template-related approaches has been done with hexagonal mesoporous silica,[57] porous anodic aluminum oxide (AAO),[58] biological species,[59] block copolymers,[60] and amphiphilic molecules.[61] Although the morphology of the nanowires can be well controlled by the utilization of this method, time consuming processing, the requirement of post-treatment to remove the template, and limitation to large scale production are considerable disadvantages. In addition, electrochemical method was chosen as another early-stage process for AgNWs synthesis; however, irregular morphology, polycrystallinity, low yield, and aspect ratio have reduced the popularity of this technique.[62] AgNWs can also be synthesized via UV irradiation method which includes the decomposition of $AgNO_3$ precursor to silver seeds (Ag^+) in the presence of a protective agent, and then formation of long AgNWs.[63] Effect of synthesis parameters on AgNW morphology have been investigated by different groups[64,65] but this approach is time consuming and not inherently industrially scalable. On the other hand, photoreduction technique, which relies on obtaining silver nanoparticles from silver nitrate film by a laser-induced photoactuation followed by fusion of nanoparticles in the template via photothermal effect, has been proposed.[66] In this method, surface morphology and size of AgNWs can be controlled by the thickness and pore diameter of the employed template, initial concentration of the silver nitrate solution, and laser operation parameters. However, relatively slow speed process and lack of mass production are noticed as drawbacks of this method.[67,77]

Since performance of the pressure sensors is highly affected by the size and morphology of the AgNWs, investigating most cost-effective synthesis method as well as optimal synthesis conditions are crucial. Polyol method has been recognized as a low-cost and simple method providing high yield comparing to the other methods. Hence, due to the disadvantages of other methods mentioned above and promising prospects of polyol method, it has been widely used in pressure sensor applications.[78]

3.1. Polyol Method

The polyol method has raised a lot of attention for generating AgNWs owing to its cost-efficiency, simplicity, and fast processing.[68–70] The polyol method is based on chemical reduction of $AgNO_3$, leading to the unidimensional growth of AgNWs by using poly(vinylpyrrolidone) (PVP) as a capping agent and ethylene glycol (EG) as a solvent and reducing agent.[79] Usually, polyol synthesis runs at high temperatures due to the high boiling point of ethylene glycol (197.3 °C), which is used to dissolve both PVP and $AgNO_3$.[78] Typically, dissolved $AgNO_3$ and PVP are pumped together by a syringe to the three-neck flask, including preheated ethylene glycol immersed in an oil bath (160–180 °C) followed by removal of byproduct nanoparticles from the final solution by centrifuge. The yield and morphology of the AgNWs synthesized in the polyol process are influenced by various factors, including $AgNO_3$ concentration, PVP concentration, PVP MW, reaction temperature, stirring speed, $AgNO_3$:PVP molar ratio, thus making the process highly tailorable.[80]

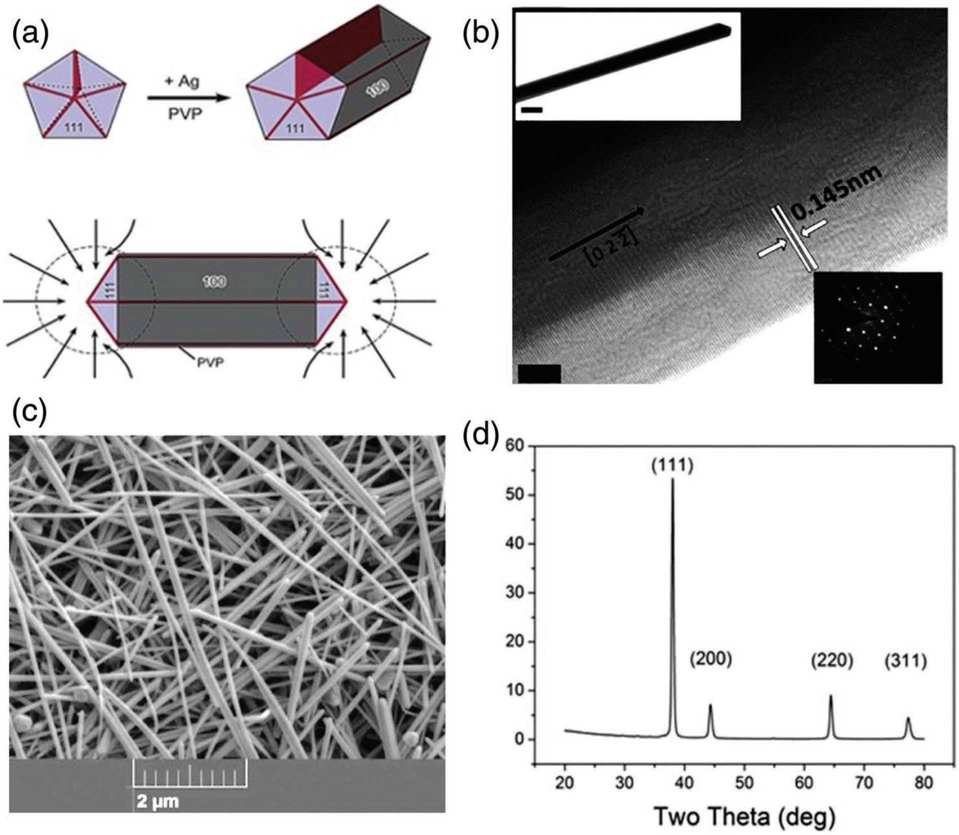

Figure 2. a) Schematic illustration of AgNWs growth mechanism. Reproduced with permission.[81] Copyright 2003, American Chemical Society. b) TEM image and electron diffraction pattern of AgNWs synthesized with polyol method. Reproduced with permission.[51] Copyright 2012, American Chemical Society. c) SEM image of AgNWs synthesized with polyol method. Reproduced with permission.[80] Copyright 2017, The Electrochemical Society. d) X-ray diffraction pattern of AgNWs synthesized with polyol method. Reproduced with permission.[51] Copyright 2012, American Chemical Society.

Understanding the growth mechanism of AgNWs is a complex task. Xia et al. proposed that AgNWs developed gradually by multiple-twinned particles (MTPs), exhibiting 5-fold symmetry as presented in **Figure 2**a.[81] Crystallization of silver atoms occurred on highly reactive twin boundaries by the growth of MTP into silver nanorods and then providing silver nanowires under twin planes action. PVP, as an important factor in the growth mechanism, passivates preferentially the {100} facets of the silver nanoparticles and facilitates the addition of silver ions to the {111} facets.[29] Typically, synthesis of AgNWs 30–60 nm in diameter and 1–50 μm in length has been successfully demonstrated via polyol synthesis method.[82] Examples of the standard morphology of the AgNWs are shown in Figure 2b,c, while the crystallinity of the AgNWs is demonstrated in Figure 2d.

3.2. Solvothermal Method

In comparison, solvothermal synthesis method, which has similar mechanism and uses the same precursors, has been investigated as an alternative to polyol synthesis owing to its simplicity, low-cost, and ease of control.[83] Typically, $AgNO_3$, PVP, ethylene glycol, and metal salts are mixed and then transferred to a Teflon lined stainless steel autoclave, followed by heating in an oven with a specific temperature and time. Various research groups investigated the impact of reaction parameters on the AgNW morphology such as PVP MW, solvent type, reducing agent and salt type.[71,84–86]

3.3. Hydrothermal Method

Consequently, hydrothermal method was introduced for AgNW synthesis, which can be recognized as a green process since water is used instead of ethylene glycol. Similar to solvothermal method, the reaction is performed in a Teflon lined stainless steel autoclave and mild reducing agent such as glucose is used instead of ethylene glycol.[76,87] Compared to other methods, AgNW synthesis with hydrothermal technique is relatively new and a systematic work investigating the reaction parameters on the morphology is not yet available.

4. Fabrication Methods for Flexible Electrodes and Dielectric Layers

4.1. Fabrication of AgNWs Based Electrodes

Coating, embedding, or patterning of AgNWs on a flexible substrate to form an electrode is a very crucial step for the

ADVANCED MATERIALS INTERFACES
www.advmatinterfaces.de

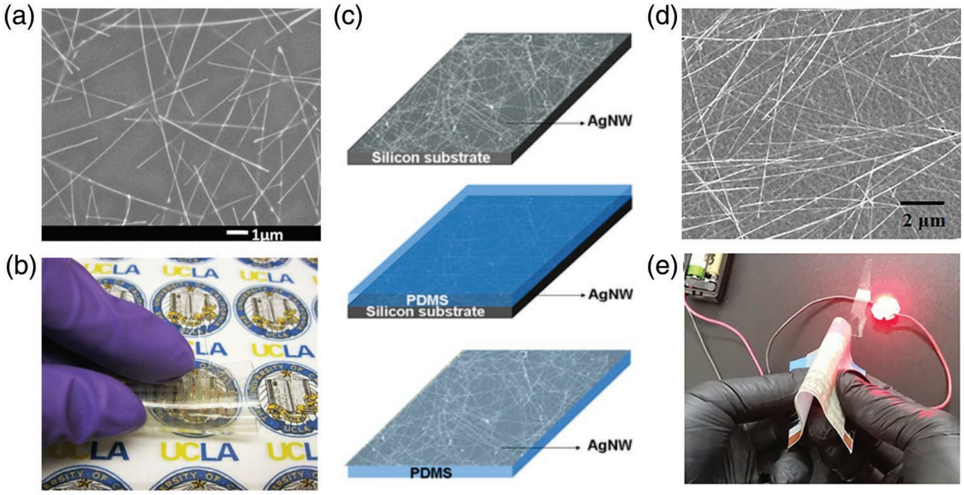

Figure 3. a) SEM image of AgNW embedded polyurethane electrode. b) Final flexible sensor with AgNW/polyurethane electrode. a,b) Reproduced with permission.[25] Copyright 2013, American Institute of Physics. c) schematic electrode fabrication process via transferring of the AgNWs to PDMS substrate. Reproduced with permission.[22] Copyright 2015, IEEE. d) SEM image of AgNW/Transparent wood electrode and e) ultimate flexible sensor. d,e) Reproduced with permission.[45] Copyright 2021, Elsevier.

fabrication of pressure sensors. In this section, we reviewed the types of electrodes and related electrode fabrication processes.

Besides that, electrode and dielectric layer are the fundamental components of a capacitive pressure sensor. They have different influence on the performance of the sensors. In addition, they have different fabrication processes. Therefore, we believe that it is highly crucial to discuss them in different sections.

4.1.1. Plain Electrode

The central idea behind plain electrode fabrication is to find out efficient ways of transferring conductive nanomaterials to flexible substrates in the form of interconnected network. A key example of this is the flexible polyurethane/AgNW electrode fabricated by Hu et al. via coating glass with AgNWs and subsequently annealing them, followed by coating with urethane liquid rubber compounds and curing it, which finally allowed the transfer of the AgNWs onto the urethane polymer surface.[25] The electrode microstructure and the final sensor with PDMS dielectric layer is shown in **Figure 3**a,b. Chen et al. Chhetry et al.,[42] and Xu et al.[88] benefited from the same approach to deposit the AgNWs on flexible PDMS substrate and the related fabrication process is displayed in Figure 3c. In addition, another approach for preparation of flexible electrode was shown via coating and transferring the AgNWs onto the PDMS substrate via vacuum filtration process.[55]

Recently, Tang et al. demonstrated flexible electrode fabrication via depositing the AgNWs on transparent wood film by Meyer rod coating.[45] The electrode microstructure and the ultimate flexible sensor is exhibited in Figure 3d,e. It is essential to note that flexible wood substrate is an exciting new alternative for the silicon or petroleum-based polymers. In their work, the wood substrate was obtained from wood veneers via delignification process, and then impregnating PEGDA, followed by curing with UV light.

4.1.2. Microstructured Electrodes

Compared to flat electrodes described in the previous subsection, microstructured electrodes can demonstrate enhanced sensitivity, owing to the localized stress at the tips of the microstructures.[9] For instance, wrinkle-like structures, based on the buckling instability of multilayer structures with mismatching mechanical properties, were introduced to PDMS substrate by stretching the substrate, followed by UV/O_3 treatment, bar coating of AgNWs and releasing to its initial length leading to wrinkle formation.[23] The uniform distribution of the AgNWs on the microstructured PDMS is shown in **Figure 4**a. Consequently, this approach was also applied to fabricate microarray structure electrodes with AgNWs by Shuai et al.[52] On the other hand, Quan et al. developed microstructured electrode by replicating the surface structure of glass with matte finish to PDMS, which was further coated with AgNWs via airbrushing.[43] Topology of this replicated PDMS substrate is depicted in Figure 4b. Consequently, pressure sensors were fabricated with these approaches and their related properties are summarized in Table 1. It is notable that replicating a micro/nanostructured surface with an elastomer offers wide range of options to prepare electrodes with different surface topographies.

An intriguing form of microstructure pattern replication draws its inspiration from biological surfaces that come with diverse surface structures. In a significant example, PDMS microtowers were prepared by replicating the inverse surface structures of lotus leaf onto PDMS.[53] Then, dense and ultrathin film of AgNWs on the microtowers was deposited with the help of the capillary flow, as illustrated in Figure 4c,d. Similarly, in another work, lotus leaves were utilized as templates for fabricating micropapillary PDMS surface.[56] On the other hand, the leaf possesses skeleton which has a network structure consisting of interconnected vein microstructures. For instance, Elsayes et al. demonstrated the use of leaf skeleton of Bodhi tree as electrode via coating of AgNWs on the

ADVANCED MATERIALS INTERFACES
www.advmatinterfaces.de

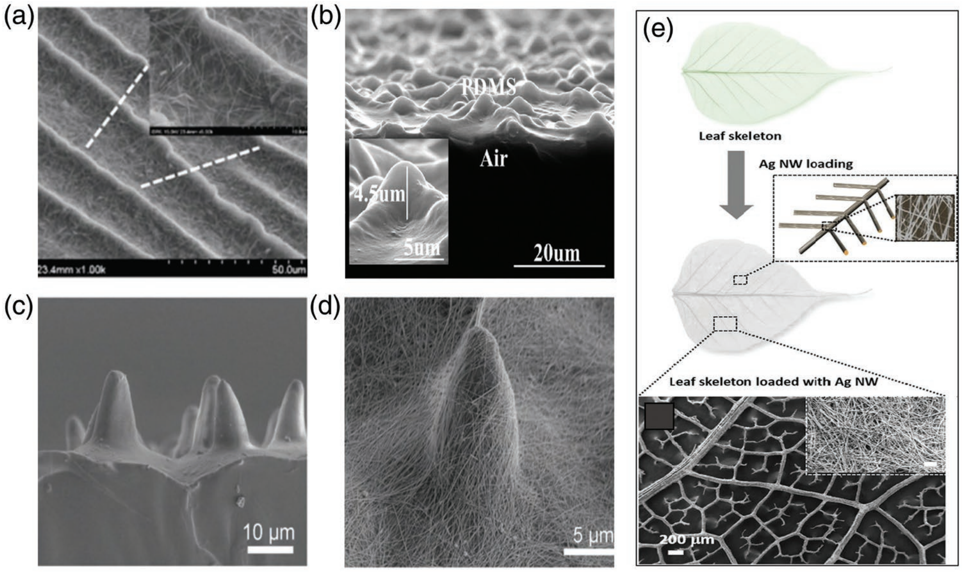

Figure 4. a) AgNW embedded buckle like microstructured electrode. Reproduced with permission.[23] Copyright 2015, Royal Society of Chemistry. b) Topology of PDMS substrate replicated from glass with matte finish. Reproduced with permission.[43] Copyright 2017, Elsevier. c) PDMS microtowers prepared from inverse replica of lotus leaf, d) AgNW coated PDMS microtowers electrode. c,d) Reproduced with permission.[53] Copyright 2018, Wiley-VCH. e) AgNW coated Bodhi tree leaf electrode. Reproduced with permission.[46] Copyright 2020, Wiley-VCH.

backbone, which provided conductive network across the leaf skeleton[46] and the electrode fabrication process in shown in Figure 4e. In addition, the same group also demonstrated the use of rubber tree leaf with the similar approach to prepare leaf-based electrode.[54] The final sensor properties of devices constructed on these biomimetic electrodes are listed in Table 1. Biomimetic approach for preparing sensor electrodes is still in its infancy stage and there are a lot of unexplored natural surfaces for replication and leaf structures as electrode substrate.

4.1.3. Porous Electrode

Sensitivity improvement of the pressure sensors has been reported with porous dielectric layers and separate flat electrodes. However, instead of separately producing dielectric and electrode layers, Cicek et al. demonstrated the fabrication of pressure sensor via deposition of AgNWs on top and bottom of a melamine sponge as a thin layer via 3D masking, and leaving the remaining part of the foam as a dielectric layer.[49] The schematic sensor structure and the uniform deposition of the AgNWs on the sponge is demonstrated in **Figure 5**a. Besides, Peng et al. presented AgNW/PDMS foam electrode via coating the AgNWs on a sugar template, followed by infiltration of PDMS and dissolving sugar.[50] The porous electrode structure and uniformly deposited AgNWs is illustrated in Figure 5b. On the other hand, porous knitted wool fabric that was coated with AgNWs was fabricated by Gurarslan et al. (Figure 5c).[48] Additionally, breathable porous electrode was fabricated by screen printing of the AgNWs on the electrospinned PVDF nanofiber membrane.[26] Figure 5d exhibits the schematic fabrication technique and SEM image of final porous electrode. The properties of the sensors with porous electrode are also shown in Table 1.

The distinct benefit of all these approaches is the simplicity of the fabrication process due to conductive and dielectric layers being inherently connected, as well as the opportunity to prepare thoroughly breathable sensors, which are desirable for wearable applications.

4.1.4. Fiber-Based Electrode

Electronic textiles (e-textiles) are very promising in flexible and wearable sensors owing to their lightweight, flexibility and comfort and achieving electrical properties at the fiber level is highly desirable for the next generation e-textiles. Therefore, integrating the conductive AgNWs in the yarns offers a facile and low-cost approach to prepare pressure sensors that are inherently integratable to textiles and can thus significantly improve the user comfort. For instance, polyurethane fiber twined by polyester yarn was dip-coated uniformly with the AgNWs to form conductive yarns[27] (**Figure 6**a,b). These yarns were assembled onto different dielectric materials in an orthogonal face-to-face configuration to form sensing pixels (Figure 6c). PDMS, Dragon skin, and Ecoflex were used as dielectric materials and the best sensor properties were obtained with Ecoflex, owing to its lower elastic modulus. The sensor structure was fabricated by placing the AgNW-coated yarns on the PDMS substrate in parallel and then pouring a liquid PDMS and curing to stack the yarns in the PDMS structure. Next, dielectric material was poured between two electrodes and allowed to cure to form the sensor structure. Consequently, in another work, fiber electrodes were fabricated via integrating the AgNWs in the bacterial cellulose via wet-spinning.[89] Then, the dielectric PDMS layer was applied via dip-coating, which provided uniform PDMS layer (Figure 6d). The wet-spinning of bacterial cellulose/AgNW solution resulted in hierarchically porous

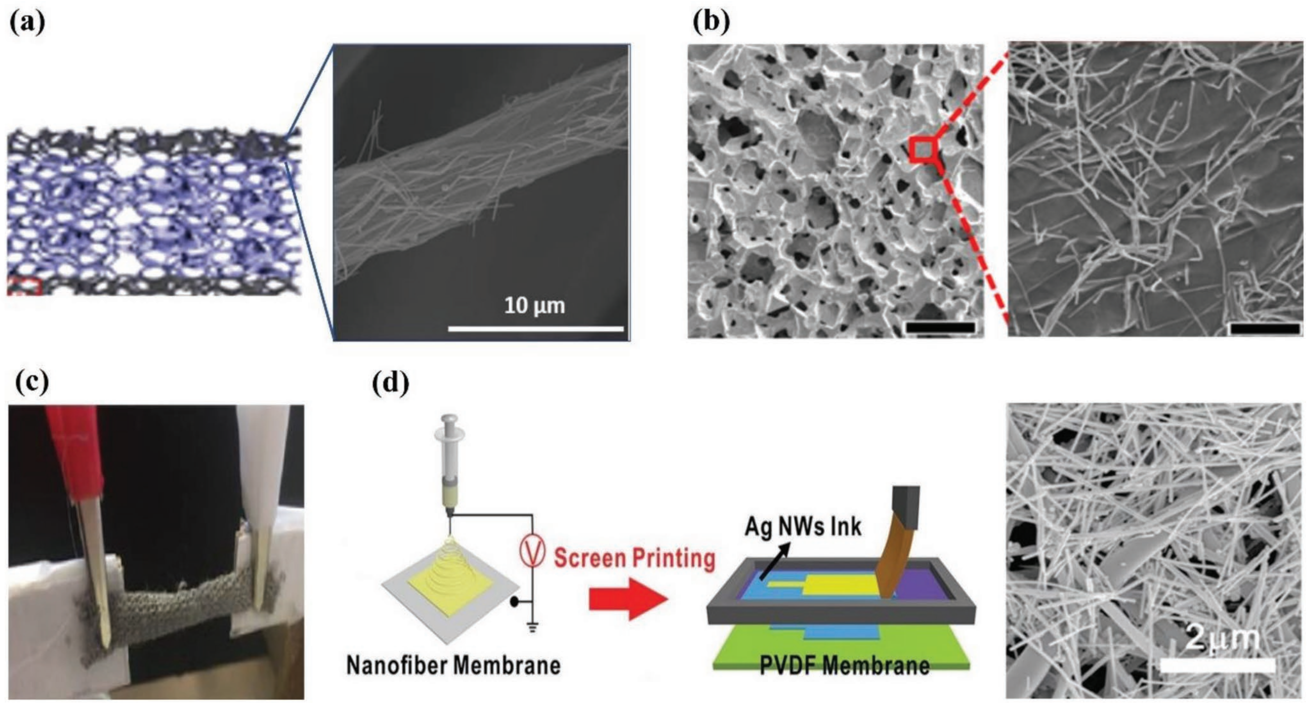

Figure 5. a) Porous AgNW/melamine sponge electrode. Reproduced with permission.[49] Copyright 2021, Wiley-VCH. b) Porous PDMS/AgNW electrode fabricated from sugar template. Reproduced with permission.[50] Copyright 2020, American Chemical Society. c) AgNW coated porous wool fabric. Reproduced with permission.[48] Copyright 2019, SAGE. d) Schematic demonstration of fabrication method and SEM image of porous electrode. Reproduced with permission.[26] Copyright 2017, Wiley-VCH.

structure with uniform distribution of AgNWs (Figure 6e). In addition, the sensing pixels were formed via assembling the fibers perpendicularly on a textile-based substrate (Figure 6f). This outstanding hierarchical structure provided high radial compressibility, which in turn led to a large capacitive change with pressure.

4.1.5. Patterned Electrode Arrays

Numerous approaches have been developed to prepare flexible capacitive pressure sensor arrays, which require the patterning of AgNWs. Since the substrates should be flexible polymer materials, the patterning techniques should not include harsh

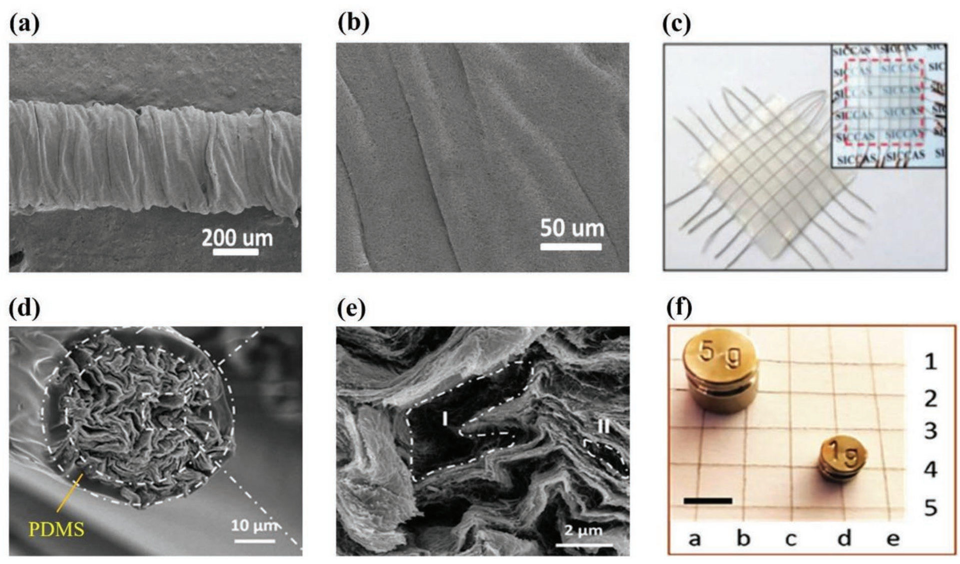

Figure 6. a) AgNW coated SCY, b) demonstration of uniform coating of AgNWs on SCY, c) photograph of the pressure sensor array with AgNW coated SCY. a–c) Reproduced with permission.[27] Copyright 2017, Royal Society of Chemistry. d) PDMS coated AgNW/bacterial cellulose fiber, e) demonstration of the hierarchical microstructure of AgNW/bacterial cellulose fiber and f) sensing pixels. d–f) Reproduced with permission.[89] Copyright 2020, American Chemical Society.

conditions, such as the inorganic counterpart processing. For instance, screen printing method was utilized to prepare 7 × 7 array with a feature size of 2 mm and PDMS as the dielectric layer, as shown in **Figure 7**a.[90] Consequently, Kim et al. fabricated 15 × 15 array sensor via parylene-C stencil patterning method, which provided line width of 500 µm.[91] Besides, Jeong et al. employed lift-off micropatterning for the construction of 16 × 16 sensor array, as illustrated in Figure 7b.[92] Additionally, Han et al. achieved 100 µm line patterns on a 5 mm × 5 mm sensor area with a technique that relies on the irradiation of light through a mask to AgNW coated PET substrate and then etching the NWs that were not exposed to light (Figure 7c).[93] Similar approach was also used by different research groups for the fabrication of sensor arrays.[47,94,95] On the other hand, spray coating of Mxene/AgNW ink through a mask was performed to obtain conductive electrodes on PDMS substrate, as shown in Figure 7d. Table 1 summarizes the sensor properties, however, it is worthy to note that, in the patterned electrode fabrication approaches, the researchers did not investigate the sensor performances in detail, but they only demonstrated capacitive pressure sensor as a proof of concept. In general, these sensor arrays can provide more information about the pressure change and distribution than a single sensor in the same area. Therefore, there are still many issues to be explored with the patterned electrode sensors, such as investigation of the sensor properties, utilization and optimization of different patterning techniques and using microstructured or porous dielectric layers.

4.2. Fabrication of AgNW-Based Dielectric Composites

Typically, easily compressible, and rapidly responding dielectric layer upon external force has a significant influence on the thickness change, which in turn leads to the capacitance change in capacitive pressure sensors. On the other hand, change of the dielectric constant with pressure is another approach to acquire capacitance change. For instance, Shi et al.[40] fabricated a dielectric layer by embedding AgNWs in microstructured PDMS layer, which was then sandwiched between two identical ITO/PET electrodes to form a pressure sensor, as shown in **Figure 8**a,b. Consequently, Zhao et al. prepared AgNW/TPU core–shell nanofiber dielectric layer via electrospinning.[41] Then, this dielectric layer was stacked between two gold/PDMS electrodes in order to assemble a pressure sensor (Figure 8c,d). Analogously, breathable flexible pressure sensor was demonstrated by integrating the electrospinned AgNW/TPU dielectric layer, the microstructure of which is shown is Figure 8e, and two CNT/TPU electrodes.[96] In another approach, porous PVA/AgNW dielectric layer was fabricated via foaming and repeated freezing and thawing.[97] Macro and microstructure of the AgNW loaded highly porous PVA foam dielectric material is displayed in Figure 8f,g. Manipulating the porosity and dielectric constant of the dielectric layer has a great influence on the sensitivity,[9] therefore, elastic and flexible foams, sponges or aerogels with tunable porosity and AgNW loading offer a wide potential in the flexible pressure sensors.

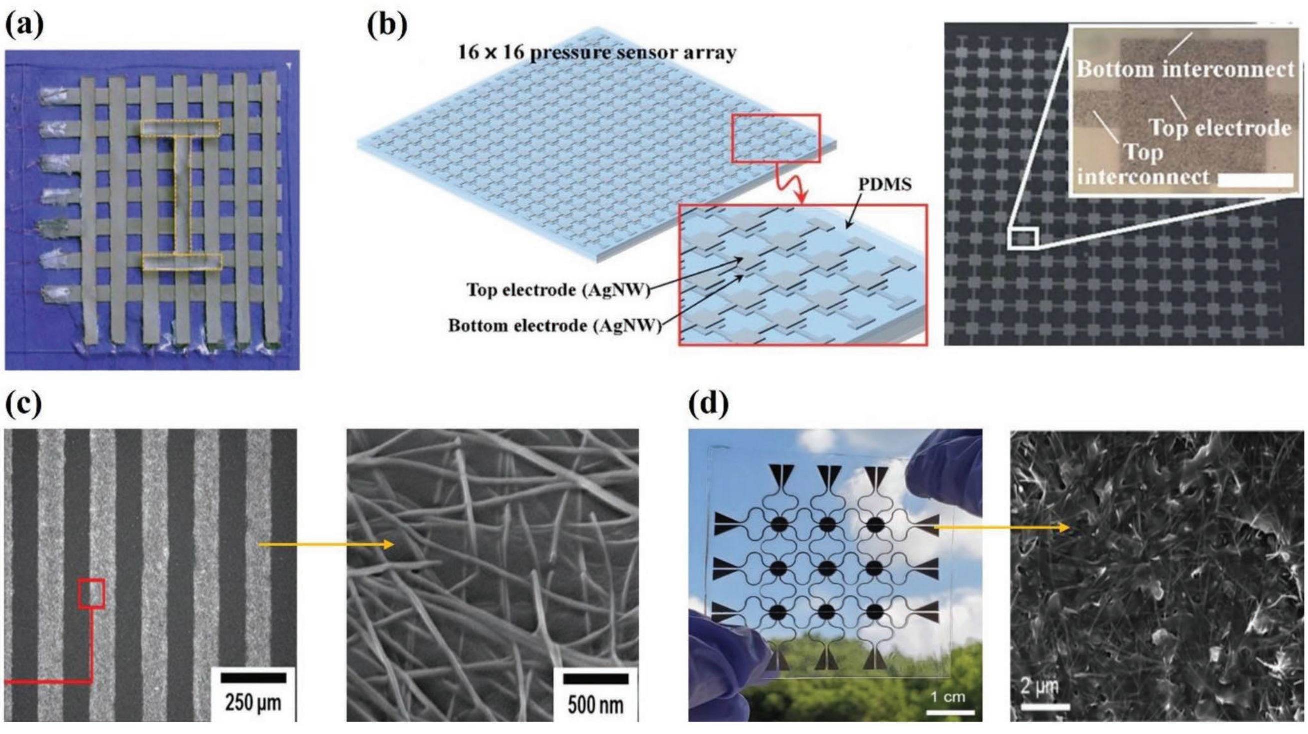

Figure 7. a) Macro image of 7 × 7 array prepared via screen printing. Reproduced with permission.[90] Copyright 2014, The Royal Society of Chemistry. b) 16×16 sensor array constructed with lift-off micropatterning approach. Reproduced with permission.[92] Copyright 2016, The Royal Society of Chemistry. c) SEM images of the AgNW lines prepared by selective light irradiation. Reproduced with permission.[93] Copyright 2017, The Royal Society of Chemistry. d) AgNW/Mxene composite electrodes on PDMS substrate prepared with spraying through mask. Reproduced with permission.[21] Copyright 2021, American Chemical Society.

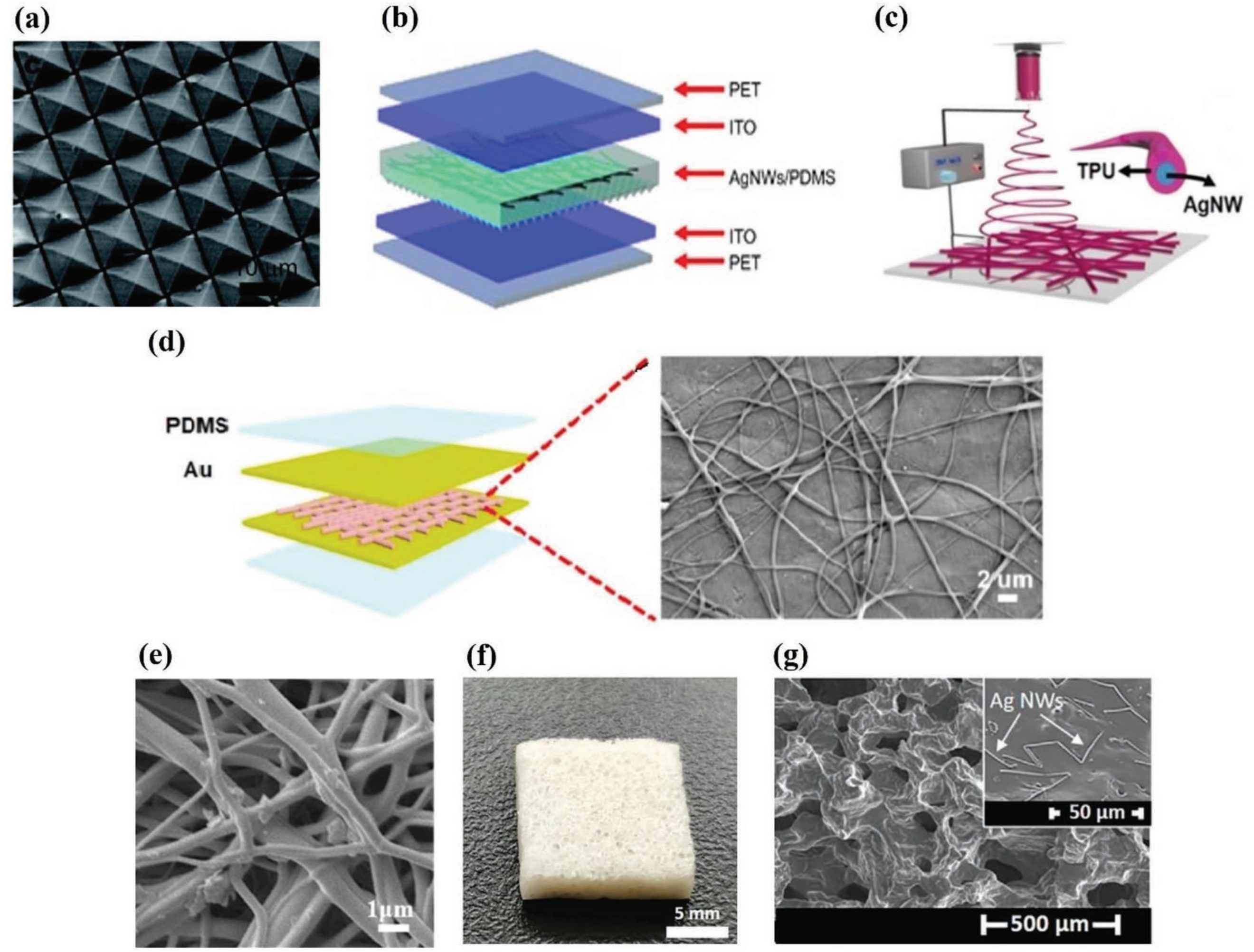

Figure 8. a) SEM image of microstructured AgNW/PDMS dielectric layer, b) structure of the flexible pressure sensor with AgNW/PDMS dielectric layer. a,b) Reproduced with permission.[40] Copyright 2018, Springer. c) Schematic illustration of the preparation of AgNW/TPU dielectric layer, d) architecture of the flexible pressure sensor with AgNW/TPU dielectric layer and SEM image of the AgNW/TPU fibers. c,d) Reproduced with permission.[41] Copyright 2020, American Chemical Society. e) SEM image of AgNW/TPU composite nanofiber dielectric layer. Reproduced with permission.[96] Copyright 2020, MDPI. f) Digital image of the fabricated porous AgNW/PVA nanocomposite dielectric layer. g) SEM image porous Ag NW/PVA nanocomposite dielectric layer. f,g) Reproduced with permission.[97] Copyright 2021, Wiley-VCH.

4.3. Computational Analysis of Sensor Designs

When it comes to computational methods, finite-elemental analysis (FEA) has typically been employed to reveal the effect of the microstructured substrate or dielectric layer on the sensing mechanism by comparing with the flat substrate or dielectric layer. For instance, Wan et al. examined the effect of microstructured substrate via replicating PDMS microtowers from lotus leaf and coated them with AgNWs (Figure 4c,d).[53] The pressure sensor was fabricated by sandwiching colorless polyimide (PI) film between AgNW coated flat PDMS and AgNW coated microtower PDMS layers. The deformation of the sensor against external pressure was simulated with FEA, as demonstrated in **Figure 9**a. External pressure resulted in stress concentrated at the contact points of the microtower array and dielectric layer. In comparison with the flat PDMS, microstructured film displayed larger local stresses and more thickness change. In addition, influence of microtower density was also simulated, which showed that less dense structure provided more thickness change. It is worthy to note that simulation results were all consistent with the experimental outputs.

On the other hand, effect of porosity on stress distribution on the sensor was elucidated by Cicek et al. via comparing the porous melamine sponge and nonporous flat PET layers by FEA analysis.[49] The simulation demonstrated that while stress was localized at the edges of the sensor body for flat PET, the stress was homogeneously distributed within the entire body for porous melamine, as shown in Figure 9b. In addition, the stress experienced with flat PET was smaller than the porous melamine, owing to the compressibility of the sponge. Therefore, sponge like materials well suits to those sensors with high sensitivity in subtle pressure regime.

Additionally, impact of microstructures in the dielectric layer was analyzed with FEA to analyze the changes in the stress and deformation under different external pressures (Figure 9c). Increased external pressure resulted in stress generation within

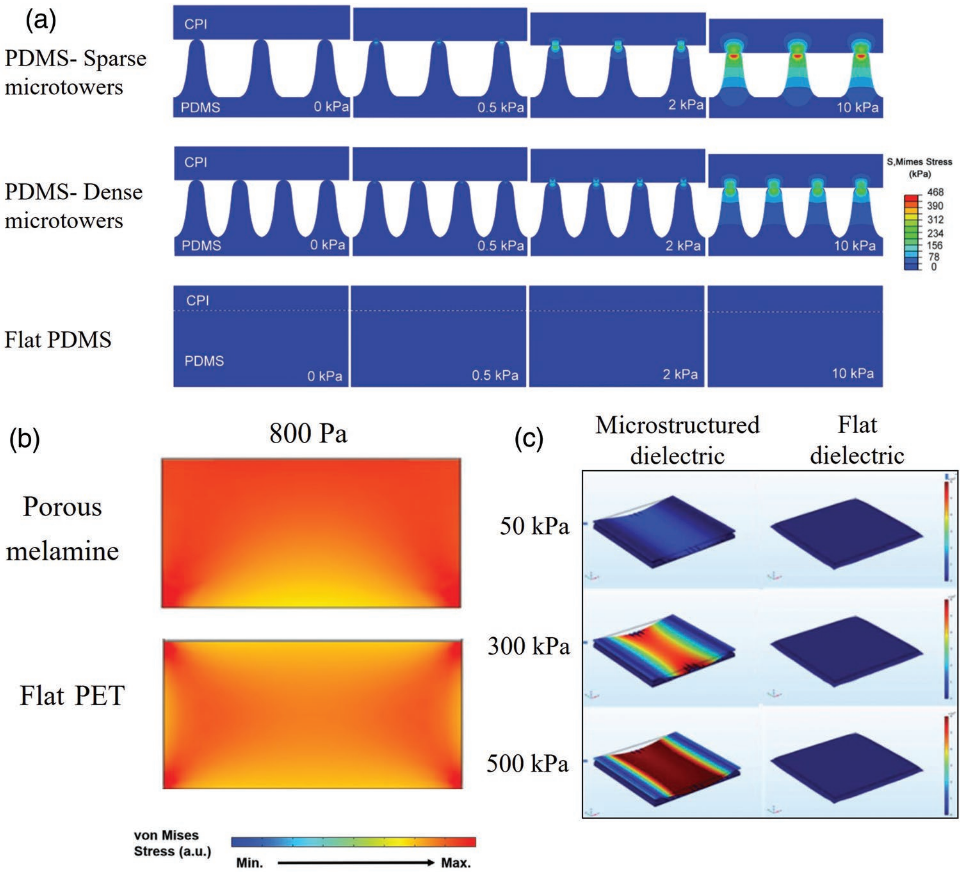

Figure 9. a) FEA simulation depicting the local stress distribution and the deformation of sparse, dense PDMS microtowers array, and flat PDMS at pressures of 0.5, 2, and 10 kPa. Reproduced with permission.[53] Copyright 2018, WILEY-VCH. b) FEA simulation results of von Mises stress distribution within porous melamine and flat PET substrate (bottom) under compressive loads of 800 Pa. Reproduced with permission.[49] Copyright 2021, WILEY-VCH. c) FEA simulation demonstrating stress distributions of the microstructured and flat dielectric sensors. Reproduced with permission.[55] Copyright 2021, Royal Society of Chemistry.

sensor body. In addition, the microstructured and flat dielectric layers displayed different stress distributions, which was attributed to the hierarchical microstructures in the dielectric layer.

Zhao et al.[41] and Chhetry et al.[42] carried out similar FEA analyzes for 3-D AgNW-TPU nanofiber dielectric layer and microstructured solid polymer electrolyte dielectric layer, respectively. These studies also generated similar conclusions that microstructured dielectric layers provided larger deformations with the external forces compared to the flat layers and the stresses typically concentrated on the tip of the microstructures. To summarize, FEA provides very crucial information regarding the material's behavior under external stress, therefore, utilizing FEA while designing microstructured or porous substrate and dielectric layers may have great impact on fabrication of highly sensitive pressure sensors.

5. Performance of the Sensors

5.1. Sensitivity

The sensitivities of the sensors prepared with AgNW based electrodes and dielectric layers on different pressure regimes are summarized in **Tables** 1 and **2**, respectively. Sensitivity (in the subtle pressure regime) of various capacitive pressure sensors prepared with AgNW based electrodes and dielectric

Table 2. Properties of the sensors prepared with AgNW based dielectric layer.

Host material	Electrode structure	AgNW length [μm]	Sensitivity [kPa^{-1}] Subtle pressure (1 Pa–1 kPa)	Low pressure (1–10 kPa)	Medium pressure (10–100 kPa)	Detection limit [Pa]	Response time [ms]	Loading/ unloading cycle	Refs.
Microstructured PDMS	ITO/PET	150	0.831	0.063	–	1.4	30	10 000 (1 kPa)	[40]
TPU nanofiber	Au/PDMS	–	1.21	0.15	–	0.9	100	10 000	[41]
Porous PVA	PVA/CNT	30	1.8862	0.1271	–	–	25	10 000	[97]

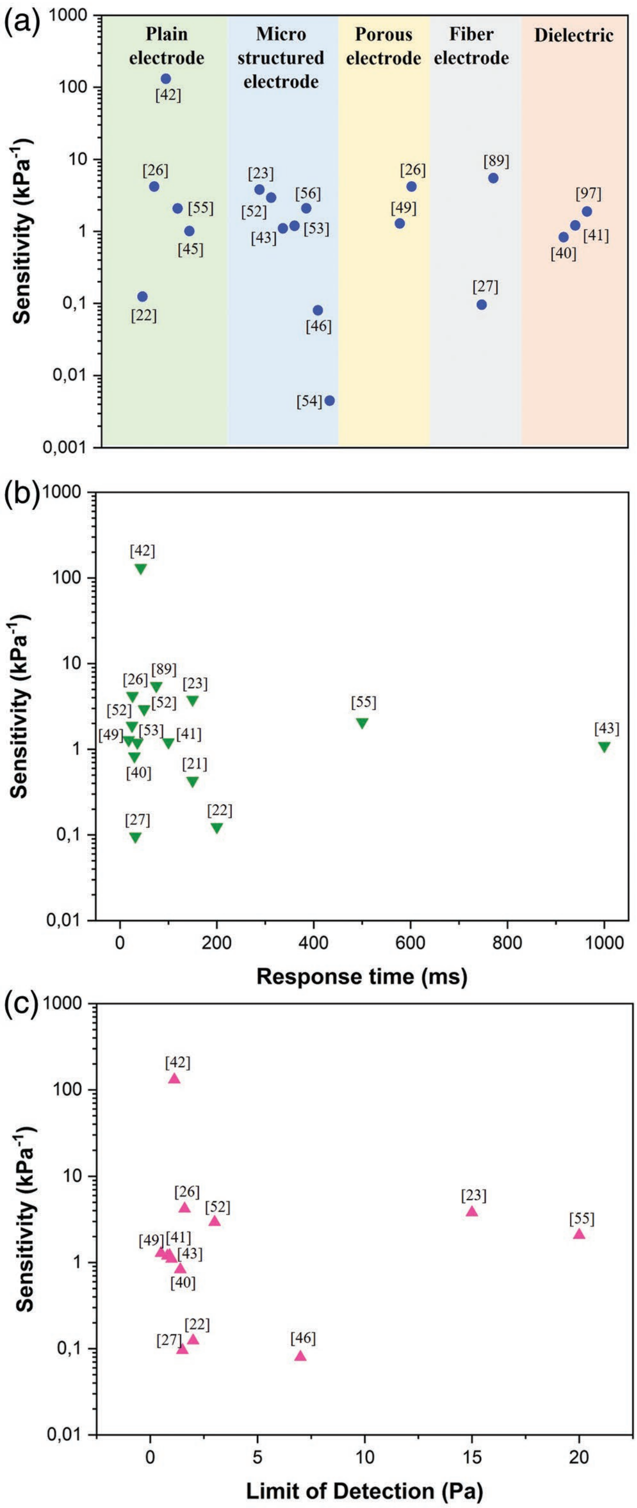

Figure 10. Properties of the pressure sensors prepared with AgNW based electrode and dielectric layer a) sensitivity, b) response time and c) limit of detection.

layers is depicted in **Figure 10**a. The sensitivity values are typically centralized in 1–10 kPa^{-1} range, which are higher than for the structures without AgNWs.[10] The highest sensitivity (131.5 kPa^{-1}) was achieved by sandwiching of a microstructured Iontronic film (dielectric layer) between two identical AgNW/PDMS plain electrodes.[42] The dielectric layer was prepared by mixing 1-ethyl-3-methylimidazolium bis(trifluoromethylsulfonyl) imide and poly(vinylidene fluoride-co-hexafluoropropylene) and spin coating on an abrasive paper, which was then followed by annealing and detaching from the paper surface. The solid polymer electrolyte indicated very high interfacial capacitance by the advantage of its mobile ions and with the external pressure, the dielectric layer presented a unique ionic-electronic contact at electrode interface, which in turn enhanced the interfacial capacitance. Besides, the lower sensitivity values (<1 kPa^{-1}) could be attributed to either nonporous/unstructured nature of PDMS[22] and Ecoflex[27] dielectric film or relatively inelastic character of dried rose petals[46] and cellulose tape[54] dielectric layer.

As noted in Table 1, the sensitivity of the sensors in the low-pressure regime are approximately ten times lower than the sensitivity values in the subtle regime. However, depending on the application, this may not be the desired property. Therefore, designing sensor structures that are highly sensitive in more than one pressure regime is of great interest.

5.2. Response Time

As demonstrated in Figure 10b, the response times of the sensors are typically less than 100 ms, which is in good agreement with the general capacitive pressure sensor values.[10] The fast response of the sensors could be explained by the elastomeric nature of the substrate or dielectric layer. On the other hand, response time is also dependent on the amount of the applied pressure, however, it was ignored by the researchers and to our knowledge, there is no systematic study available addressing this issue. In addition, Figure 10b clearly displays the relationship between the sensitivity and response time of the sensor. Typically, we can say that the sensors with highest sensitivities in subtle pressure regime possess shorter response times. Besides, the high response time of the sensors presented by Chen and Guo (200 ms),[22] Liu et al. (500 ms),[55] and Quan et al. (1000 ms)[43] could be attributed to the robust and/or thick substrate and dielectric layers.

5.3. Dynamic Durability

As summarized in Tables 1 and 2, number of cycles were varied in the range of 10–100000 with different applied pressures. It is notable that the researchers typically utilized single pressure and loading/unloading frequency. However, fatigue or irreversible deformation of the sensor can depend on both the amount of applied pressure and loading/unloading frequency. Varying these parameters and then investigation of their impact on the sensor performance degradation has commonly been disregarded in the literature. On the other hand, bendability is an important performance criterion in sensor performance and long-term dynamic durability. Even though, fabrication of flexible or wearable sensor was claimed in the literature, bendability test of the entire sensor system has often been ignored or limited to few bending angles.

5.4. Limit of Detection

As shown in Figure 10c, the LOD of the AgNW based sensors are typically in the range of 1–3 Pa, which demonstrates the easy compressibility of the fabricated sensors. The relationship between the sensitivity and LOD is apparent and the sensors with higher sensitivity have lower LOD values. However, the high LOD values shown by Joo et al.[23] (15 Pa) and Liu et al.[55] (20 Pa) can be explained by the relatively lower elastic nature of the dielectric films like PMMA and natural bamboo leaves, respectively.

6. Emerging Applications

Sensor technology has gained much attention due to the fast improvement of value-added smart materials, e-textiles, intelligent home and internet of things (IoT) technology.[98] Various applications derived from pressure sensors can be divided into three main categories of human–machine interface, electronic skin, and healthcare monitoring/human motion detection, presented in this section.[7] There are still several challenges and obstacles to be solved for increasing the future prospects of these applications.

6.1. Human–Machine Interface

Communication between humans and machines is assisted by integrated devices and software. In other words, a flexible pressure sensor can play a pivotal role in translating mechanical movements of humans to electrical signals for the machine's control.[99] For instance, Guan et al. developed fiber-based highly sensitive sensors (shown in Figure 6f) for determining weak signals from human body and highly accurate pulse waves. Owing to the recognition of spatial movement of an object resulting from proximity sensitivity, a touchless piano (the playing of which doesn't require pressing the keys) is illustrated in **Figure 11**a.[89] Meanwhile, chocker sensor attached to a necklace that could detect human speech was also demonstrated in the same work. On the other hand, Zhao et al. utilized pressure sensor with AgNW/TPU nanofiber dielectric layer embedded between identical Au/PDMS layers (shown in Figure 8d) to realize human-machine interfaces.[41] They fabricated a complex piano glove with 10 independent sensors including ten basic notes for playing the piano as shown in Figure 11b. The sensors were connected to the circuit board and the change in capacitance signal was transmitted to the mobile phone application via the Bluetooth module. Furthermore, Shi et al. used the sensor shown in Figure 8b in a wearable touch keyboard to realize the human–computer interaction.[40] As illustrated in Figure 11c, the wearable keyboard system relies on the capacitance change of the sensors and transmission of the related signal to the microprocessor and then to the wireless data transmitter. Moreover, Chen et al. enabled the control of shooting video game with the help of sensors mounted on human fingers that are connected to a data acquisition (DAQ) circuit board.[100]

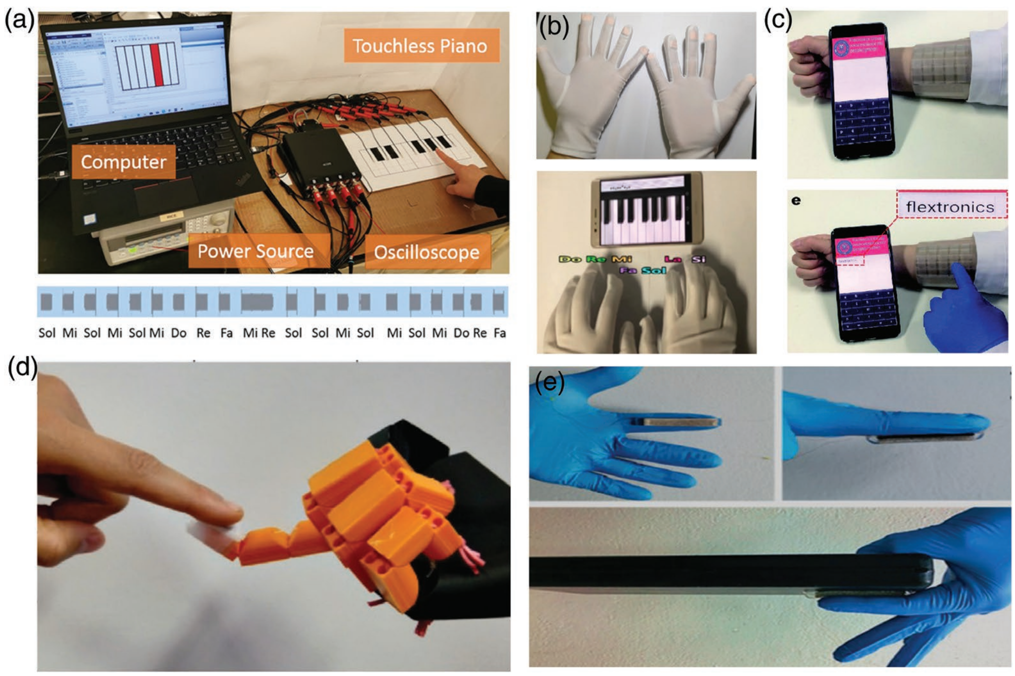

Figure 11. a) Touchless piano played with a human finger. Reproduced with permission.[89] Copyright 2020, American Chemical Society. b) Image of the data glove with 10 independent sensors and demonstration of playing the piano in the mobile app. Reproduced with permission.[41] Copyright 2020, American Chemical Society. c) Flexible sensor functioning as wearable keyboard and real-time inputting word "flextronics". Reproduced with permission.[40] Copyright 2018, Springer Nature. d) Sensor mounted on a robotic hand. Reproduced with permission.[46] Copyright 2020, Wiley-VCH. e) Force monitoring with the pressure sensor placed onto a human fingertip. Reproduced with permission.[50] Copyright 2020, American Chemical Society.

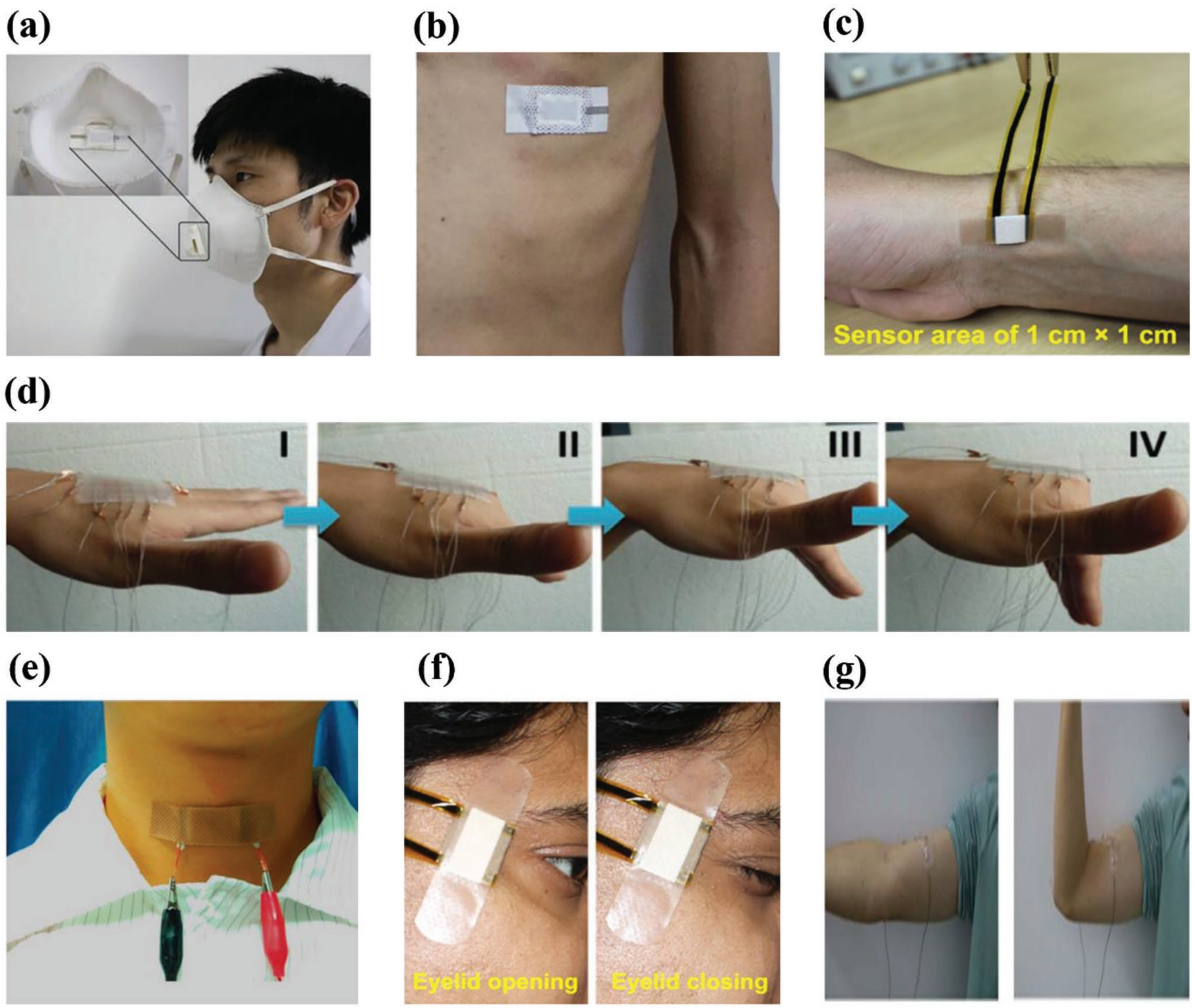

Figure 12. a) Pressure sensor attached to the mask for respiration monitoring, b) sensor attached to the chest for heart rate monitoring. a,b) Reproduced with permission.[26] Copyright 2017, WILEY-VCH. c) Sensor mounted on the radial artery for real-time monitoring of the wrist pulse. Reproduced with permission.[42] Copyright 2018, American Chemical Society. d) Palm bending with different angles. Reproduced with permission.[27] Copyright 2017, Royal Society of Chemistry. e) Sensor placed on human neck to detect the vocal cords vibration. Reproduced with permission.[52] Copyright 2017, American Chemical Society. f) Sensor detecting muscle movement during eyelid opening and closing. Reproduced with permission.[42] Copyright 2018, American Chemical Society. g) Sensor mounted on human arm to detect arm bending. Reproduced with permission.[103] Copyright 2021, IOP Publishing.

6.2. Electronic Skin

Different sensing functionalities of human skin can be simulated by various flexible electronic skin constructions.[7] The pressure sensor is an essential element of electronic skin, requiring flexibility, conformability and small sensing pixels.[26] Besides pressure sensing, different functionalities, such as self-healing ability, multi-stimuli differentiation and temperature sensing can also be integrated into E-skins.[101] To actualize the pressure sensing E-skin, Elsayes et al. mounted the leaf electrode-based sensor (Figure 4e) at the fingertip of a 3D-printed robotic hand, as exhibited in Figure 11d, and it was demonstrated that the sensor was able to detect human finger's touching the robotic hand.[46] In addition, Peng et al. placed the fabricated pressure sensor on the tip of a human finger that could detect and determine the applied force for the application of human–machine interface (Figure 11e).[50] Moreover, Ho et al. demonstrated the utilization of a crack-enhanced pressure sensor for 2D color mapping of simultaneous external load sensing as well as detecting human motions, such as slow muscle movement.[102]

By and large, skin-like pressure sensors have attracted significant attention because of their ultraflexibility, which can be widely used in wearable applications. However, air permeability is one of the remaining important challenges of skin-like pressure sensors. To overcome this issue, Yang et al.

developed cost-effective, lightweight and breathable pressure sensors from nanofiber membranes as a promising candidate for electronic skin applications. The mentioned pressure sensor consists of AgNW coated PVDF nanofiber membrane as electrode and TPU nanofiber membrane as dielectric material.[26]

6.3. Healthcare Monitoring and Human Motion Detection

Flexible pressure sensors attached to the human body can detect physiological parameters and they provide an opportunity for continuous healthcare monitoring and human motion detection.[3] For instance, AgNW based pressure sensor was successfully implemented to monitor the human respiration and heart rate as illustrated in **Figure 12**a,b.[26] Additionally, Figure 12c demonstrates the utilization of pressure sensor mounted on radial artery for real-time monitoring of the wrist pulse.[42] On the other hand, human motion detection, such as finger bending,[27] voice recognition,[52] eye blinking,[42] and arm bending[103] was successfully demonstrated with the flexible pressure sensors, as displayed in Figure 12d–g. Furthermore, similar human motion detection was also detected with the AgNW based pressure sensors fabricated by Yao and Zhu[90] Cicek et al.,[49] Li et al.,[44] Nie et al.,[56] Liu et al.,[55] and Che et al.[94] However, there is an uncertainty about long terms stability of the pressure sensors at daily working conditions, which needs more research and exploration in the future.[24]

7. Conclusions and Outlook

Herein, we have summarized recent progress of AgNW based flexible capacitive pressure sensors and their usage in emerging technologies. The fabrication methods of AgNW based electrode and dielectric layers were classified and we highlight that AgNWs are not only a good electrode material but also a good filler material in the dielectric layer, which can be explained by their outstanding flexibility, electrical conductivity, and high dielectric constant. We then compared the sensor performances including sensitivity, response time, dynamic durability, and limit of detection. Proper selection of substrate and dielectric material and adding microstructures or porosity to them can have strong impact on the sensor performance. Considering the application perspective, these sensors show promising results in emerging technologies including human-machine interface, electronic skin, healthcare monitoring and human motion detection.

However, realization of sensors with low detection limit and high sensitivity in the ultralow pressure (<1 Pa) is still a significant challenge, specifically in healthcare monitoring applications. Even though there have been achievements in sensor performance in subtle pressure (1 Pa–1 kPa) regime, to our knowledge highly sensitive sensors in both subtle and low-pressure regime relevant to human motion detection or healthcare monitoring have not been reported yet. Therefore, new material design with optimized porosity and microstructures are highly desired. In addition, the effect of nanowire length on the sensor performance has not been investigated in detail yet. The mechanical and electrical integrity of the sensors under dynamic bending still needs further investigation. Yet, the fabricated sensors' dimensions are small and until now, the fabrication processes are commonly optimized only using methods typical for low to medium technology-readiness level. Large scale production approaches thus remain as a challenge for the commercialization of the sensors. We believe that established printing techniques combined with AgNW inks are very promising for the commercialization of the sensors. Another bottleneck is the use of rigid wiring systems for the data acquisition from the sensors rendering long-term pressure monitoring in skin mountable devices still a grand challenge. Regarding the emerging applications, combination of the sensors with artificial intelligence and internet of things is only emerging in the literature. In addition to pressure, sensors that can detect other signals such as temperature, strain, and biological fluids need for further research effort to enable both early detection and monitoring of diseases for advanced healthcare monitoring applications.

Acknowledgements

This research was funded by H2020-MSCA-IF-2020 with a grant number of 101031327 (WEARSENSNANO) as well as by ERC StG project 949648 "ModelCom."

Conflict of Interest

The authors declare no conflict of interest.

Keywords

capacitive flexible pressure sensor, dielectric, electrode, emerging applications, silver nanowires

Received: April 19, 2022
Revised: June 29, 2022
Published online: September 14, 2022

[1] F. Xu, X. Li, Y. Shi, L. Li, W. Wang, L. He, R. Liu, *Micromachines* **2018**, *9*, 580.
[2] F. He, X. You, W. Wang, T. Bai, G. Xue, M. Ye, *Small Methods* **2021**, *5*, 2001041.
[3] T. Q. Trung, N.-E. Lee, *Adv. Mater.* **2016**, *28*, 4338.
[4] Y. Zang, F. Zhang, C. Di, D. Zhu, *Mater. Horiz.* **2015**, *2*, 140.
[5] Y. Gu, T. Zhang, H. Chen, F. Wang, Y. Pu, C. Gao, S. Li, *Nanoscale Res. Lett.* **2019**, *14*, 263.
[6] A. M. Almassri, W. Z. Wan Hasan, S. A. Ahmad, A. J. Ishak, A. M. Ghazali, D. N. Talib, C. Wada, *J. Sens.* **2015**, *2015*, 846487.
[7] Y. Huang, X. Fan, S. Chen, N. Zhao, *Adv. Funct. Mater.* **2019**, *29*, 1808509.
[8] Y. Kim, J. H. Oh, *Appl. Sci.* **2020**, *10*, 6403.
[9] R. Li, Q. Zhou, Y. Bi, S. Cao, X. Xia, A. Yang, S. Li, X. Xiao, *Sens. Actuators, A* **2021**, *321*, 112425.
[10] R. B. Mishra, N. El-Atab, A. M. Hussain, M. M. Hussain, *Adv. Mater. Technol.* **2021**, *6*, 2001023.

[11] Q.-J. Sun, T. Li, W. Wu, S. Venkatesh, X.-H. Zhao, Z.-X. Xu, V. A. L. Roy, *ACS Appl. Electron. Mater.* **2019**, *1*, 711.
[12] Z. Yin, M.-J. Yin, Z. Liu, Y. Zhang, A. P. Zhang, Q. Zheng, *Adv. Sci.* **2018**, *5*, 1701041.
[13] N. Yogeswaran, S. Gupta, R. Dahiya, in *2018 IEEE SENSORS*, IEEE, Piscataway, NJ **2018**, pp. 1–4.
[14] Mordor Intelligence, *Capacitive Pressure Sensor Market - Growth, Trends, Covid-19 Impact, and Forecasts (2022 - 2027)*, **2020**, https://www.mordorintelligence.com/industry-reports/global-capacitive-pressure-sensors-market-industry (accessed: August 2022).
[15] M. Zou, Y. Ma, X. Yuan, Y. Hu, J. Liu, Z. Jin, *J. Semicond.* **2018**, *39*, 11010.
[16] M. Han, J. Lee, J. K. Kim, H. K. An, S.-W. Kang, D. Jung, *Sens. Actuators, A* **2020**, *305*, 111941.
[17] X. Fu, J. Zhang, J. Xiao, Y. Kang, L. Yu, C. Jiang, Y. Pan, H. Dong, S. Gao, Y. Wang, *Nanoscale* **2021**, *13*, 18780.
[18] L. Huang, H. Wang, D. Zhan, F. Fang, *IEEE Sens. J.* **2021**, *21*, 12048.
[19] J. Yang, S. Luo, X. Zhou, J. Li, J. Fu, W. Yang, D. Wei, *ACS Appl. Mater. Interfaces* **2019**, *11*, 14997.
[20] X. He, X. He, H. He, S. Liang, Z. Liu, J. Liang, Y. Xin, W. Yang, Y. Chen, C. Zhang, *ACS Omega* **2021**, *6*, 27208.
[21] X.-F. Zhao, X.-H. Wen, S.-L. Zhong, M.-Y. Liu, Y.-H. Liu, X.-B. Yu, R.-G. Ma, D. W. Zhang, J.-C. Wang, H.-L. Lu, *ACS Appl. Mater. Interfaces* **2021**, *13*, 45924.
[22] S. Chen, X. Guo, *IEEE Trans. Nanotechnol.* **2015**, *14*, 619.
[23] Y. Joo, J. Byun, N. Seong, J. Ha, H. Kim, S. Kim, T. Kim, H. Im, D. Kim, Y. Hong, *Nanoscale* **2015**, *7*, 6208.
[24] W. Chen, X. Yan, *J. Mater. Sci. Technol.* **2020**, *43*, 175.
[25] W. Hu, X. Niu, R. Zhao, Q. Pei, *Appl. Phys. Lett.* **2013**, *102*, 083303.
[26] W. Yang, N.-W. Li, S. Zhao, Z. Yuan, J. Wang, X. Du, B. Wang, R. Cao, X. Li, W. Xu, Z. L. Wang, C. Li, *Adv. Mater. Technol.* **2018**, *3*, 1700241.
[27] Y. Cheng, R. Wang, H. Zhai, J. Sun, *Nanoscale* **2017**, *9*, 3834.
[28] L. Hu, H. Wu, Y. Cui, *MRS Bull.* **2011**, *36*, 760.
[29] F. Basarir, F. S. Irani, A. Kosemen, B. T. Camic, F. Oytun, B. Tunaboylu, H. J. Shin, K. Y. Nam, H. Choi, *Mater. Today Chem.* **2017**, *3*, 60.
[30] F. Oytun, V. Kara, O. Alpturk, F. Basarir, *Thin Solid Films* **2017**, *636*, 40.
[31] H. J. Shin, F. Oytun, J. W. Kim, B. R. Lee, J. Y. Kim, F. Basarir, H. Choi, *Electrochim. Acta* **2020**, *337*, 135839.
[32] F. Oytun, O. Alpturk, F. Basarir, *Mater. Res. Bull.* **2019**, *112*, 53.
[33] B. Tugba Camic, F. Oytun, M. Hasan Aslan, H. Jeong Shin, H. Choi, F. Basarir, *J. Colloid Interface Sci.* **2017**, *505*, 79.
[34] B. T. Camic, H. I. Jeong, M. H. Aslan, A. Kosemen, S. Kim, H. Choi, F. Basarir, B. R. Lee, *Nanomaterials* **2020**, *10*, 46.
[35] B. Tugba Camic, H. Jeong Shin, M. Hasan Aslan, F. Basarir, H. Choi, *J. Colloid Interface Sci.* **2018**, *512*, 158.
[36] C. Altinkok, F. Oytun, F. Basarir, M. A. Tasdelen, *J. Photochem. Photobiol., A* **2017**, *346*, 479.
[37] S. Coskun, B. Aksoy, H. E. Unalan, *Cryst. Growth Des.* **2011**, *11*, 4963.
[38] H. Jiang, K. S. Moon, F. Hua, C. P. Wong, *Chem. Mater.* **2007**, *19*, 4482.
[39] P. Alivisatos, *Nat. Biotechnol.* **2004**, *22*, 47.
[40] R. Shi, Z. Lou, S. Chen, G. Shen, *Sci. China Mater.* **2018**, *61*, 1587.
[41] S. Zhao, W. Ran, D. Wang, R. Yin, Y. Yan, K. Jiang, Z. Lou, G. Shen, *ACS Appl. Mater. Interfaces* **2020**, *12*, 32023.
[42] A. Chhetry, J. Kim, H. Yoon, J. Y. Park, *ACS Appl. Mater. Interfaces* **2019**, *11*, 3438.
[43] Y. Quan, X. Wei, L. Xiao, T. Wu, H. Pang, T. Liu, W. Huang, S. Wu, S. Li, Z. Chen, *J. Alloys Compd.* **2017**, *699*, 824.
[44] W. Li, L. Xiong, Y. Pu, Y. Quan, S. Li, *Nanoscale Res. Lett.* **2019**, *14*, 183.
[45] Q. Tang, M. Zou, L. Chang, W. Guo, *Chem. Eng. J.* **2022**, *430*, 132152.
[46] A. Elsayes, V. Sharma, K. Yiannacou, A. Koivikko, A. Rasheed, V. Sariola, *Adv. Sustainable Syst.* **2020**, *4*, 2000056.
[47] B. Zhang, Z. Xiang, S. Zhu, Q. Hu, Y. Cao, J. Zhong, Q. Zhong, B. Wang, Y. Fang, B. Hu, J. Zhou, Z. Wang, *Nano Res.* **2014**, *7*, 1488.
[48] A. Gurarslan, B. Özdemir, İ. H. Bayat, M. B. Yelten, G. Karabulut Kurt, *J. Eng. Fibers Fabr.* **2019**, *14*, 1558925019856222.
[49] M. O. Cicek, D. Doganay, M. B. Durukan, M. C. Gorur, H. E. Unalan, *Adv. Mater. Technol.* **2021**, *6*, 2001168.
[50] S. Peng, S. Wu, Y. Yu, B. Xia, N. H. Lovell, C. H. Wang, *ACS Appl. Mater. Interfaces* **2020**, *12*, 22179.
[51] J. H. Lee, P. Lee, D. Lee, S. S. Lee, S. H. Ko, *Cryst. Growth Des.* **2012**, *12*, 5598.
[52] X. Shuai, P. Zhu, W. Zeng, Y. Hu, X. Liang, Y. Zhang, R. Sun, C. Wong, *ACS Appl. Mater. Interfaces* **2017**, *9*, 26314.
[53] Y. Wan, Z. Qiu, Y. Hong, Y. Wang, J. Zhang, Q. Liu, Z. Wu, C. F. Guo, *Adv. Electron. Mater.* **2018**, *4*, 1700586.
[54] A. Koivikko, V. Lampinen, K. Yiannacou, V. Sharma, V. Sariola, *IEEE Sens. J.* **2021**, *22*, 11241.
[55] Z. Liu, T. Liang, Y. Xin, J. Huang, J. Liang, X. He, C. Zhang, W. Yang, X. He, *RSC Adv.* **2021**, *11*, 17291.
[56] K. Nie, Z. Wang, H. Zhou, R. Tang, X. Shen, Q. Sun, *J. Mater. Chem. C* **2020**, *8*, 16113.
[57] J. Y. Piquemal, G. Viau, P. Beaunier, F. Bozon-Verduraz, F. Fiévet, *Mater. Res. Bull.* **2003**, *38*, 389.
[58] L. B. Kong, M. Lu, M. K. Li, H. L. Li, X. Y. Guo, *J. Mater. Sci. Lett.* **2003**, *22*, 701.
[59] S. Behrens, J. Wu, W. Habicht, E. Unger, *Chem. Mater.* **2004**, *16*, 3085.
[60] D. Zhang, L. Qi, J. Ma, H. Cheng, *Chem. Mater.* **2001**, *13*, 2753.
[61] D. M. Eisele, H. V. Berlepsch, C. Böttcher, K. J. Stevenson, D. A. Vanden Bout, S. Kirstein, J. P. Rabe, *J. Am. Chem. Soc.* **2010**, *132*, 2104.
[62] Y. Shi, L. He, Q. Deng, Q. Liu, L. Li, W. Wang, Z. Xin, R. Liu, *Micromachines* **2019**, *10*, 330.
[63] H. Abdullah, K. J. Kadhim, I. H. Hilal, *World Sci. News* **2016**, *37*, 220.
[64] K. Zou, X. H. Zhang, X. F. Duan, X. M. Meng, S. K. Wu, *J. Cryst. Growth* **2004**, *273*, 285.
[65] L. Liu, C. He, J. Li, J. Guo, D. Yang, J. Wei, *New J. Chem.* **2013**, *37*, 2179.
[66] N. M. Abbasi, H. Yu, L. Wang, Zain-Ul-Abdin, W. A. Amer, M. Akram, H. Khalid, Y. Chen, M. Saleem, R. Sun, J. Shan, *Mater. Chem. Phys.* **2015**, *166*, 1.
[67] Y. H. Lin, K. T. Chen, J. R. Ho, *Jpn. J. Appl. Phys.* **2011**, *50*, 065002.
[68] Y. Sun, Y. Xia, *Adv. Mater.* **2002**, *14*, 833.
[69] Y. Sun, B. Gates, B. Mayers, Y. Xia, *Nano Lett.* **2002**, *2*, 165.
[70] Y. Sun, Y. Yin, B. T. Mayers, T. Herricks, Y. Xia, *Chem. Mater.* **2002**, *14*, 4736.
[71] Y. Li, S. Guo, H. Yang, Y. Chao, S. Jiang, C. Wang, *RSC Adv.* **2018**, *8*, 8057.
[72] S. Chen, Y. Guan, Y. Li, X. Yan, H. Ni, L. Li, *J. Mater. Chem. C* **2017**, *5*, 2404.
[73] Z. Hu, C. Kong, Y. Han, H. Zhao, Y. Yang, H. Wu, *Mater. Lett.* **2007**, *61*, 3931.
[74] J. Xu, J. Hu, C. Peng, H. Liu, Y. Hu, *J. Colloid Interface Sci.* **2006**, *298*, 689.
[75] Z. Wang, J. Liu, X. Chen, J. Wan, Y. Qian, *Chem. - Eur. J.* **2005**, *11*, 160.
[76] H. W. Jang, Y. H. Kim, K. W. Lee, Y. M. Kim, J. Y. Kim, *APL Mater.* **2017**, *5*, 080701.
[77] W. B. Zhao, J. J. Zhu, H. Y. Chen, *J. Cryst. Growth* **2003**, *258*, 176.
[78] S. Hemmati, M. T. Harris, D. P. Barkey, *J. Nanomater.* **2020**, *2020*, 6.
[79] J. Jiu, K. Murai, D. Kim, K. Kim, K. Suganuma, *Mater. Chem. Phys.* **2009**, *114*, 333.

[80] S. Hemmati, D. P. Barkey, *ECS J. Solid State Sci. Technol.* **2017**, *6*, P132.
[81] Y. Sun, B. Mayers, T. Herricks, Y. Xia, *Nano Lett.* **2003**, *3*, 955.
[82] K. E. Korte, S. E. Skrabalak, Y. Xia, *J. Mater. Chem.* **2008**, *18*, 437.
[83] B. Liu, H. Yan, S. Chen, Y. Guan, G. Wu, R. Jin, L. Li, *Nanoscale Res. Lett.* **2017**, *12*, 212.
[84] Y. Zhang, J. Guo, D. Xu, Y. Sun, F. Yan, *ACS Appl. Mater. Interfaces* **2017**, *9*, 25465.
[85] Q. Xue, W. Yao, J. Liu, Q. Tian, L. Liu, M. Li, Q. Lu, R. Peng, W. Wu, *Nanoscale Res. Lett.* **2017**, *12*, 480.
[86] Y. Li, Y. Li, Z. Fan, H. Yang, X. Yuan, C. Wang, *ACS Omega* **2020**, *5*, 18458.
[87] D. Sharma, D. A. Rakshana, R. M. Balakrishnan, P. E. Jagadeeshbabu, *Mater. Res. Express* **2019**, *6*, 075050.
[88] F. Xu, Y. Zhu, *Adv. Mater.* **2012**, *24*, 5117.
[89] F. Guan, Y. Xie, H. Wu, Y. Meng, Y. Shi, M. Gao, Z. Zhang, S. Chen, Y. Chen, H. Wang, Q. Pei, *ACS Nano* **2020**, *14*, 15428.
[90] S. Yao, Y. Zhu, *Nanoscale* **2014**, *6*, 2345.
[91] Y. Kim, N. Chou, S. Kim, in *2015 IEEE SENSORS*, IEEE, Piscataway, NJ **2015**, pp. 1–3.
[92] D.-W. Jeong, N.-S. Jang, K.-H. Kim, J.-M. Kim, *RSC Adv.* **2016**, *6*, 74418.
[93] C. J. Han, B.-G. Park, M. S. Oh, S.-B. Jung, J.-W. Kim, *J. Mater. Chem. C* **2017**, *5*, 9986.
[94] Q. Che, Q. Zhao, M. Hu, R. Qin, G. Shan, J. Yang, *ACS Appl. Nano Mater.* **2021**, *4*, 12726.
[95] S. Lim, J.-M. Oh, B. Yoo, C. J. Han, B.-J. Lee, M. S. Oh, J.-W. Kim, *Appl. Surf. Sci.* **2021**, *561*, 149989.
[96] J. Wang, Y. Lou, B. Wang, Q. Sun, M. Zhou, X. Li, *Sensors* **2020**, *20*, 2459.
[97] P. Wang, G. Li, J. Liu, Z. Hou, C. Meng, S. Guo, C. Liu, S. Fan, *Adv. Mater. Interfaces* **2021**, *8*, 2100998.
[98] F. Xu, X. Li, Y. Shi, L. Li, W. Wang, L. He, R. Liu, *Micromachines* **2018**, *9*, 580.
[99] H. Zhao, Y. Zhou, S. Cao, Y. Wang, J. Zhang, S. Feng, J. Wang, D. Li, D. Kong, *ACS Mater. Lett.* **2021**, *3*, 912.
[100] S. Chen, S. Peng, W. Sun, G. Gu, Q. Zhang, X. Guo, *Adv. Mater. Technol.* **2019**, *4*, 1800681.
[101] X. Wang, L. Dong, H. Zhang, R. Yu, C. Pan, Z. L. Wang, *Adv. Sci.* **2015**, *2*, 1500169.
[102] D. H. Ho, R. Song, Q. Sun, W.-H. Park, S. Y. Kim, C. Pang, D. H. Kim, S.-Y. Kim, J. Lee, J. H. Cho, *ACS Appl. Mater. Interfaces* **2017**, *9*, 44678.
[103] L. Mo, X. Meng, J. Zhao, Y. Pan, Z. Sun, Z. Guo, W. Wang, Z. Peng, C. Shang, S. Han, K. Hu, M. Cao, Y. Chen, Z. Xin, J. Lu, L. Li, *Flexible Printed Electron.* **2021**, *6*, 014001.

Fevzihan Basarir is currently working as Marie Curie fellow in the Department of Chemistry and Materials Science at Aalto University. He has received his M.Sc. and Ph.D. degree in materials science from Gwangju Institute of Science and Technology (GIST) in 2004 and 2011, respectively. He has coauthored more than 25 papers in international journals. His research interest includes synthesis and assembly of nanomaterials for flexible pressure, strain, and temperature sensors.

Zahra Madani received her M.Sc. in fibers and polymer engineering from Aalto University in 2021. Currently, she is a Ph.D. candidate in multifunctional materials design research group (MMD) under supervision of Prof. Jaana Vapaavuori at Aalto University. Her research interests focus on polymer chemistry, smart textiles and developing novel actuators for artificial muscle application.

Jaana Vapaavuori (Department of Chemistry and Materials Science, Aalto University) received her Ph.D. in Applied Physics in 2013. She leads Multifunctional Materials Design Group, established in 2019. She has received multiple recognitions, including Banting Postdoctoral Fellowship (Canada), the Young Researcher of the Year 2020 award of Finnish Foundation of Technology Promotion, and ERC Starting grant of European Research Council. Her research interests involve developing new designed materials for light-controllable nanostructures, liquid crystals, multifunctional porous materials, biomaterial-based light management layers for photovoltaics and sustainable material solutions for sensors, as well as for electrochemical devices.